Modeling and Simulation of an Industrial Trickle-Bed Reactor for Benzene Hydrogenation: Model Validation against Plant Data

ARTICLE *in* INDUSTRIAL & ENGINEERING CHEMISTRY RESEARCH · FEBRUARY 2009

Impact Factor: 2.59 · DOI: 10.1021/ie801411n

4 AUTHORS, INCLUDING:

Ville Alopaeus
Aalto University
146 PUBLICATIONS **907** CITATIONS
SEE PROFILE

Sami Toppinen
Neste Jacobs, Finland
13 PUBLICATIONS **160** CITATIONS
SEE PROFILE

Modeling and Simulation of an Industrial Trickle-Bed Reactor for Benzene Hydrogenation: Model Validation against Plant Data

Jonas Roininen,*,† Ville Alopaeus,† Sami Toppinen,‡ and Juhani Aittamaa‡

Department of Biotechnology and Chemical Technology, Helsinki University of Technology, Post Office Box 6100, FI-02015 TKK, Finland, and Neste Jacobs Oy, Post Office Box 310, FI-06101 Porvoo, Finland

A heterogeneous three-phase reactor model is used to simulate an industrial trickle-bed reactor for benzene hydrogenation, and simulated temperature profiles are compared to actual plant data. The agreement of model predictions with measured data is excellent. Analysis of the results shows that the process is limited by gas−liquid mass transfer of hydrogen. The simulation results show high sensitivity toward the liquid film mass transfer coefficient k_La. Some correlations for k_La are tested, and their validity is evaluated. The estimated values of k_La and k_Ga are comparable to measured values from a bench-scale reactor reported in the literature.

Introduction

Trickle-bed reactors are fixed-bed reactors with concurrent gas−liquid downward flow at low superficial velocities. They are used widely in the oil refining industry, typically for hydrogenation reactions such as hydrogenation of aromatics and hydrodesulfurization. Early models of trickle-bed reactors were based on pseudohomogeneous kinetics.[1,2] Korsten and Hoffmann[3] presented a three-phase heterogeneous model for the hydrodesulfurization of vacuum gas oil in a trickle-bed reactor and used it to simulate a high-pressure pilot plant. Toppinen et al.[4] presented a rigorous trickle-bed reactor model that takes into account multicomponent mass transfer effects. They simulated an industrial toluene hydrogenation reactor, however, without any validation against experimental or plant data. Avraam and Vasalos[5] have published a similar model that additionally takes into account partial wetting of the catalyst and gas-phase reaction.

In past years, there have been many studies with simulations of industrial trickle-bed hydrotreating units employing similar three-phase heterogeneous models.[6−9] Many models reported in the literature were successfully applied to simulations of pilot-plant reactors. However, the validation data for different reactors and reaction systems, especially at the industrial scale, are scarce.[9] In this work, we aim to meet this demand by comparing simulation results to data from an industrial trickle-bed reactor in a benzene hydrogenation unit.

Experimental Procedures

Industrial Unit. The present model was used to simulate an existing industrial benzene hydrogenation unit at an oil refinery in northern Europe. The unit is used for dearomatization of the benzene-rich hexane fraction from a gasoline desulfurization unit. The hydrogenation unit comprises the trickle-bed reactor and a flash tank for the separation of the gas−liquid mixture. The reactor operates adiabatically, and part of the liquid product is recycled back to the reactor for temperature control. The flow sheet of the process and its representation as a simulation model in the process simulator FLOWBAT,[10] which was used for the simulations, are shown in Figure 1.

The feed to the unit consists of 3−5 wt % benzene and some inert hydrocarbons, mainly isohexane (about 50 wt %). The hydrogenation reaction takes place on a silica-supported nickel catalyst. Side reactions, such as cracking, are not expected due to the mild conditions (temperature less than 100 °C). The flow rate of the hydrocarbon feed varies between about 40 000 and 60 000 kg·h^{-1}. The gas feed is about 1000 kg·h^{-1} and contains small amounts of hydrocarbon in addition to hydrogen (about 95 mol %). The flow rate of the recycle stream varies between 50 000 and 60 000 kg·h^{-1}. The product is virtually benzene-free. The main operational parameters of the reactor unit are given in Table 1. The reactor is equipped with staggered temperature measurement points, which are arranged helically around the reactor axis, so that a temperature profile is obtained. A complication that arises when dealing with industrial trickle-bed reactors is that the exact height of the catalyst bed is not known. The height of the catalyst bed may decrease during operation due to crushing and reorganization of catalyst particles. Here we have estimated the volume of the catalyst bed by assuming the bulk density reported by the catalyst supplier and multiplying it by the total mass of the catalyst. The height was then calculated by dividing the volume by the cross-sectional area of the bed. This situates the first temperature measurement point right at the top of the catalyst bed. This seems reasonable, since the temperature at that point is almost identical with the temperature measured at the reactor inlet.

To demonstrate the prediction capability of the model, we have chosen two illustrative operation conditions for which data were available (designated as cases 1 and 2 below). These were chosen so that they would roughly represent the range of operation encountered at the plant. The operation conditions and feed compositions for the two cases are given in Table 2. The composition of the hydrogen feed for both cases is given in Table 3. The feed compositions were determined from routine laboratory analyses made at the plant.

The data are chosen to represent the situation in a fresh catalyst bed that has reached a stable mode of operation (i.e., possible start-up transients are over, but the catalyst has not yet deactivated significantly). The data were collected within 1 month from start-up, compared to 3−5 years of total catalyst lifetime. On fresh catalyst, the reaction takes place in the first third of the length of the catalyst bed. However, the reactor is designed to take into account catalyst deactivation due to poisoning, and therefore the excess length.

Trickle-Bed Reactor Model. We used the trickle-bed reactor model of Toppinen et al.,[4] which has been implemented in FLOWBAT.[10] The model equations are discussed here very

* Corresponding author. E-mail: jonas.roininen@tkk.fi.
† Helsinki University of Technology.
‡ Neste Jacobs Oy.

10.1021/ie801411n CCC: $40.75
Published on Web 01/05/2009

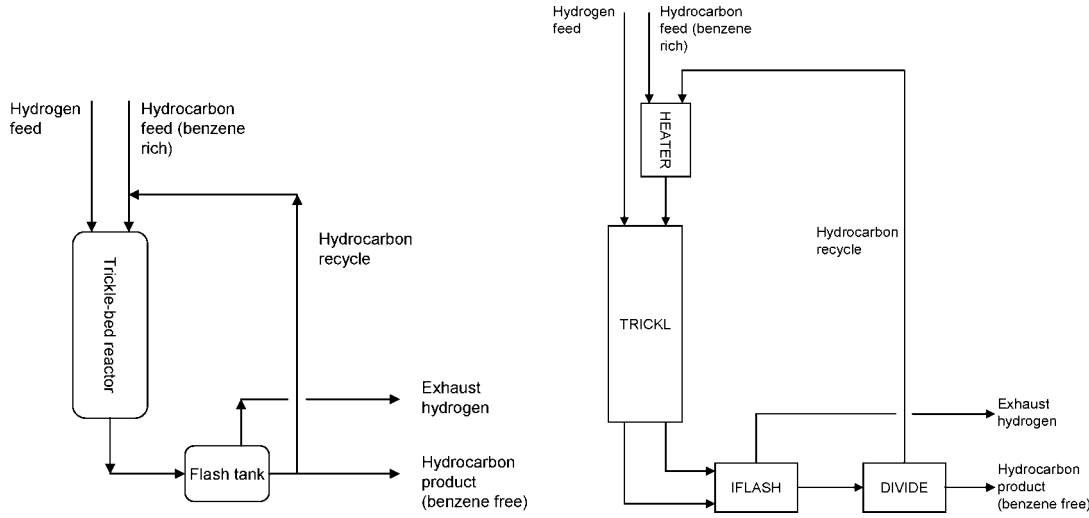

Figure 1. Flow sheet of the benzene dehydrogenation unit (left) and its representation in the process simulator FLOWBAT (right). Simulation modules: HEATER, isothermal flash with one mixed-phase outlet stream; TRICKL, trickle-bed reactor model with interfacial mass transfer; IFLASH, isothermal flash with gas and liquid outlet streams; DIVIDE, stream divider.

Table 1. Main Operational Parameter Values Used in the Simulation

Bed	
bulk density	700 kg m^{-3}
void fraction	0.4
length	5.8 m
diameter	2 m
Catalyst	
nominal size	1.2 mm
sphericity	0.874

Table 2. Feed Compositions, Flow Rates, and Temperatures for the Two Simulation Cases

	case 1	case 2
Feed Composition (wt %)		
benzene	3.6	5.1
cyclohexane	5.1	4.8
isopentane	0.2	0.3
n-pentane	6.4	4.2
isohexane	48.2	52.0
cyclopentane	3.1	3.1
n-hexane	26.1	26.0
isoheptane	7.3	4.5
Stream Flow Rates ($kg \cdot h^{-1}$)		
hydrocarbon feed	47 900	39 250
hydrogen feed	1192	1093
recycle stream	49 500	58 700
Temperature (°C)		
feed temperature	70.05	72.45

briefly; a detailed description of the model can be found in Toppinen et al.[4] The differential equations for the reactor model are as follows.

Mass balances in gas and liquid phases:

$$\frac{d\dot{n}_{Li}}{d\xi} = V_R(N_{GLi}a_{GL} - N_{LSi}a_S) \quad (1)$$

$$\frac{d\dot{n}_{Gi}}{d\xi} = -V_R N_{GLi}a_{GL} \quad (2)$$

Energy balances:

$$\frac{d\dot{E}_L}{d\xi} = V_R(q_{GL}a_{GL} - q_{LS}a_S - q_W a_W) \quad (3)$$

Table 3. Composition of Hydrogen Feed Assumed in the Simulations

component	mol %
hydrogen	89
methane	2.1
ethane	2.6
propane	2.4
isobutane	0.9
n-butane	0.6
isopentane	0.4
n-pentane	0.2
n-hexane	1.8

$$\frac{d\dot{E}_G}{d\xi} = -V_R q_{GL}a_{GL} \quad (4)$$

Pressure drop:

$$\frac{dP}{d\xi} = f(n_{Li}, n_{Gi}, T_L, T_G, P) \quad (5)$$

The steady-state mass balance for the solid catalyst phase is

$$N_{LSi}a_S + r_i = 0 \quad (6)$$

The rate r_i is assumed to be a function of the temperature and concentrations at the catalyst surface. Diffusion or heat transfer limitations inside catalyst particles are ignored or they are assumed to be included in the kinetic relations.

Mass Transfer Model. Two mass transfer models have been implemented in the FLOWBAT code: a rigorous Maxwell−Stefan mass transfer model and a simplified effective diffusivity model. Toppinen et al.[4] showed that the effective diffusivity model is reasonably accurate in this case. They argued that this is due to two reasons: First, hydrogen is the only reacting component that exists in large amounts in the gas phase and is therefore the only component that is transferred notably through the gas−liquid interface. Second, in the liquid phase both hydrogen and benzene have low concentrations, which makes the effect of total flux on the mass transfer rate insignificant. Our own simulations also showed that the results from both models are virtually identical. Because the effective diffusivity model leads to considerable saving in simulation time, we have decided to use it in the simulations below.

With the effective diffusivity method, the mass transfer flux through a film is

$$N_{\mathrm{LS}i}a_{\mathrm{S}} = k_{i,\mathrm{eff}}a_{\mathrm{S}}(c_{\mathrm{B}i} - c_{\mathrm{I}i}) \quad (7)$$

where the mass transfer coefficient is obtained from the effective diffusivity of the component. The mass transfer coefficient is calculated from an empirical correlation, which usually involves the Schmidt number, *Sc*, and hydrodynamic characteristics of the flow. The effective diffusivities are calculated with the equation[11]

$$D_{i,\mathrm{eff}} = (1 - x_i)/\sum_{\substack{j=1 \\ j\neq i}}^{n} (x_j/Đ_{ij}) \quad (8)$$

At the gas−liquid interface, the mass transfer fluxes are given by the following equations:

$$N_{\mathrm{GL}i}a_{\mathrm{GL}} = \frac{(c_{\mathrm{G}i}/K_i^*) - c_{\mathrm{L}i}}{[1/(K_i^* k_{\mathrm{G}i,\mathrm{eff}}a_{\mathrm{GL}})] + (1/k_{\mathrm{L}i,\mathrm{eff}}a_{\mathrm{GL}})} \quad (9)$$

$$K_i^* = \frac{c_{\mathrm{GI}i}}{c_{\mathrm{LI}i}} = \frac{c_{\mathrm{Gt}}}{c_{\mathrm{Lt}}}K(x_i, y_i, T_{\mathrm{avg}}, P) \quad (10)$$

The interfacial temperature and the energy flux are then calculated from

$$\alpha_{\mathrm{G}}(T_{\mathrm{G}} - T_{\mathrm{I}}) - \alpha_{\mathrm{L}}(T_{\mathrm{I}} - T_{\mathrm{L}}) + \sum_{i=1}^{n} N_{\mathrm{GL}i}(\bar{H}_{\mathrm{G}i} - \bar{H}_{\mathrm{L}i}) = 0 \quad (11)$$

At the liquid−solid interface, the equations are

$$k_{\mathrm{LS}i,\mathrm{eff}}(c_{\mathrm{L}i} - c_{\mathrm{S}i}) - N_{\mathrm{LS}i} = 0 \quad (12)$$

for mass transfer and

$$\alpha_{\mathrm{LS}}(T_{\mathrm{L}} - T_{\mathrm{S}}) + \sum_{i=1}^{n} N_{\mathrm{LS}i}\bar{H}_{\mathrm{L}i} = 0 \quad (13)$$

for the energy balance of the catalyst phase.

Liquid-phase diffusion coefficients were calculated with the Vignes,[12] Kooijman and Taylor,[13] and Wilke and Chang[14] equations. Liquid film mass transfer coefficients at the gas−liquid interface and on the catalyst surface were computed with the correlations of Goto and Smith.[15] Gas film mass transfer coefficients were calculated with the correlation of Yaici et al.[16] Heat transfer coefficients were estimated by use of the Chilton−Colburn analogy.[17] Vapor−liquid and gas−liquid equilibria at the gas−liquid interface (*K* in eq 10) were calculated with the Graboski and Daubert modification of the Soave−Redlich−Kwong equation.[18]

Kinetics. Metaxas and Papayannakos[19] tested different kinetic models for benzene hydrogenation in a bench-scale reactor and found that they all performed almost equally well. The hydrogenation reaction is strongly mass-transfer-limited, and thus the choice of the mass transfer correlation is much more important, as will be shown below. We used the kinetic expression of Toppinen et al.[20] for the mechanism with dissociative adsorption of hydrogen with parameters estimated for the heterogeneous reactor model (Table 4 in their publication). The values of the parameters are given in Table 4. The rate expression is

Table 4. Kinetic Parameters Used in the Simulation

$k_1(T_0)$	1.3	mol $s^{-1}kg^{-1}$
T_0	373.15	K
E_a	53.9	$kJmol^{-1}$
K_B	1.83 × 10^{-3}	m^3mol^{-1}
K_H	7.0745	m^3mol^{-1}

Table 5. Average Superficial Velocities, Densities, and Holdup in the Reactor

	case 1	case 2
average liquid superficial velocity (m/s)	0.014	0.014
average gas superficial velocity (m/s)	0.023	0.021
average liquid density (kg/m^3)	608	605
average gas density (kg/m^3)	7.13	7.68
average total holdup	0.27	0.21

$$R = \frac{k_1 K_{\mathrm{B}} K_{\mathrm{H}} c_{\mathrm{B}} c_{\mathrm{H}}}{(3K_{\mathrm{B}}c_{\mathrm{B}} + \sqrt{K_{\mathrm{H}}c_{\mathrm{H}}} + 1)^3} \quad (14)$$

where

$$k_1 = k_1(T_0)\exp\left[-\frac{E_a}{R}\left(\frac{1}{T} - \frac{1}{T_0}\right)\right] \quad (15)$$

Holdup, Pressure Drop, and Flow Regime. The pressure drop was set manually to a measured value of 25 kPa and a linear pressure profile was assumed. Compared to the total pressure in the reactor (1.665 MPa at the inlet), the pressure drop is almost negligible and has very little effect on the simulation results. The static holdup was calculated with the correlation of Sáez and Carbonell[21] and the dynamic holdup with the correlation of Ellman et al.[22] The average superficial velocities, densities, and total liquid holdup are shown in Table 5.

Trickle-bed reactors can operate in three flow regimes: low interaction or trickle flow regime, high interaction or pulsing flow regime, and the transition regime between these two. By use of the modified Charpentier and Favier flow chart of Larachi et al.,[23] the studied reactor was found to operate in the high interaction regime but close to the regime boundary. Recently, Urseanu et al.[24] have investigated the flow regime transition in a cumene−hydrogen system at elevated pressures. Although their data do not cover the conditions encountered in our reactor, extrapolation of their results suggests that it operates right at the boundary of the low and the high interaction regimes, or in the transition regime. This has consequences for the mass transfer correlation used, as shown below.

Results and Discussion

Comparison of the temperature measurements with the simulation results in Figure 2 shows excellent agreement of simulations with measured data. We wish to point out that there were no parameters in the kinetic model or the mass transfer correlations fitted specifically to this case. The liquid, gas, and solid temperatures are practically indistinguishable, mostly

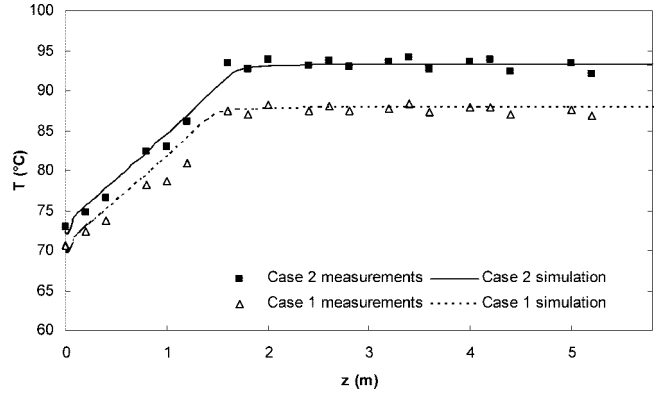

Figure 2. Comparison of measured and simulated reactor temperature profiles (simulated liquid temperatures).

Table 6. Estimated Mass and Heat Transfer Coefficients for Simulations Shown in Figure 2[a]

Mass Transfer Coefficients (s^{-1})

		$k_{Li,eff}a_{GL}$		$k_{Gi,eff}a_{GL}$		$k_{LSi,eff}a_{LS}$	
	compd	inlet	outlet	inlet	outlet	inlet	outlet
case 1	H_2	0.0428	0.0473	7.25	6.77	1.54	1.86
case 1	benzene	0.0326	0.0362	6.97	5.99	1.07	1.31
case 1	cyclohexane	0.0312	0.0356	6.85	5.87	1.01	1.23
case 2	H_2	0.0436	0.0490	10.3	8.56	1.59	1.98
case 2	benzene	0.0331	0.0373	9.93	7.37	1.10	1.38
case 2	cyclohexane	0.0316	0.0356	9.76	7.22	1.04	1.29

Heat Transfer Coefficients ($kW \cdot m^{-3} \cdot K^{-1}$)

	$\alpha_L a_{GL}$		$\alpha_G a_{GL}$		$\alpha_S a_{LS}$	
	inlet	outlet	inlet	outlet	inlet	outlet
case 1	277	258	347	362	9940	10 200
case 2	275	253	488	464	10 020	10 200

[a] Values for $k_{Li,eff}$ and $k_{LSi,eff}$ were calculated with the correlations of Goto and Smith.[15] Values for $k_{Gi,eff}$ were calculated with the correlation of Yaici et al.[16]

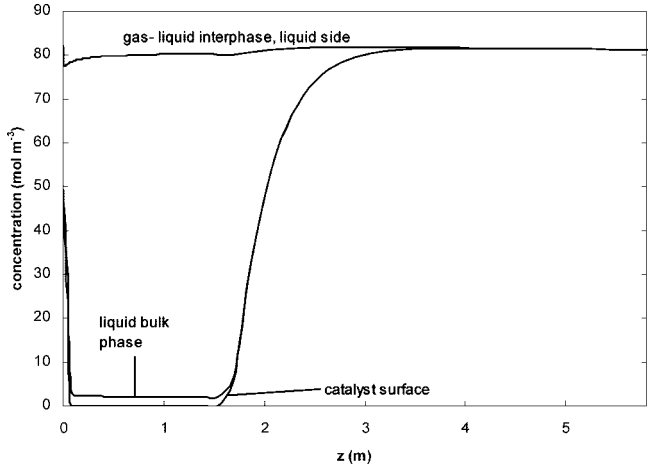

Figure 3. Hydrogen concentrations at the liquid side of the gas−liquid interface, in the liquid bulk phase, and at the catalyst surface (case 2).

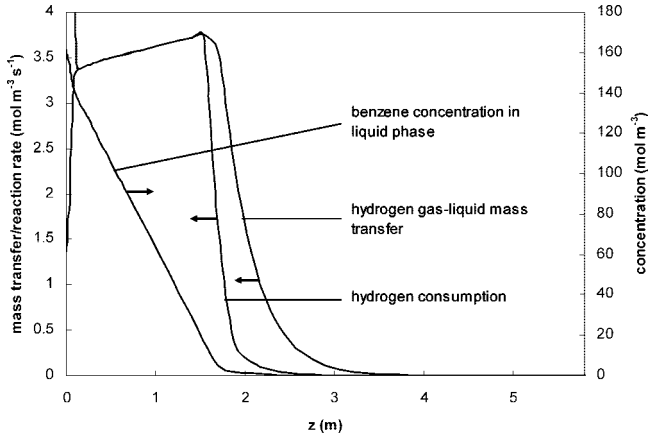

Figure 4. Hydrogen mass transfer, hydrogen consumption, and benzene concentration in the liquid phase (case 2).

within 0.1 K, indicating that catalyst−liquid and liquid−gas heat transfer is very good. Since the reactor is adiabatic and benzene reacts to almost 100%, the outlet temperature is mainly determined by the amount of benzene in the feed, the heat of reaction, and the recycle ratio. The inlet temperature was adjusted to match the measured temperature of the two-phase

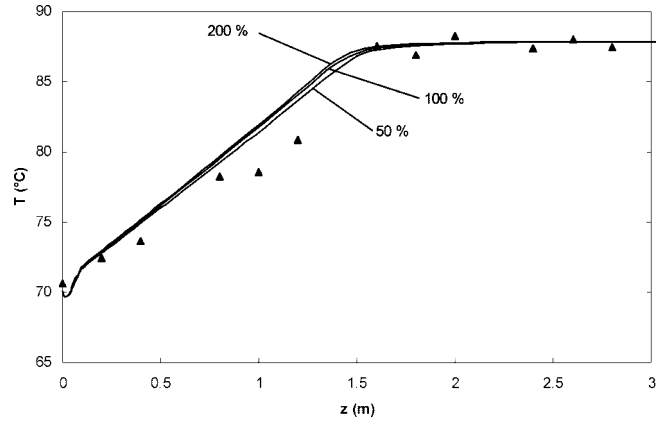

Figure 5. Effect of $k_{LSi}a$ values scaled to 50% and 200% of calculated value on the simulated temperature profile (case 1; ▲, measured values).

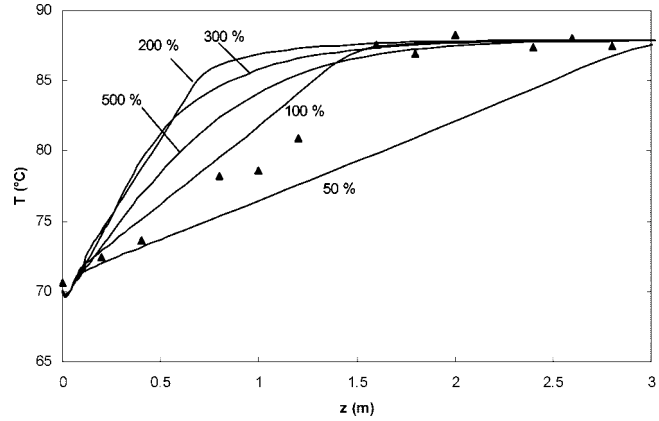

Figure 6. Effect of $k_{Li}a$ values scaled to 50%, 200%, 300%, and 500% of calculated value on the simulated temperature profile (case 1; ▲, measured values).

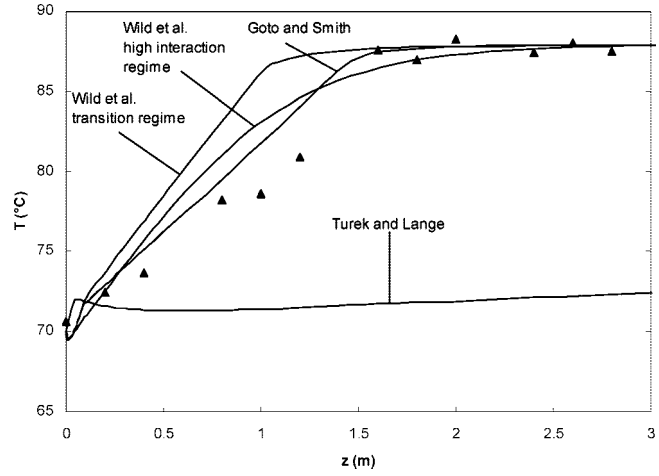

Figure 7. Effect of the choice of different correlations for $k_{Li}a$ on the simulated temperature profile (case 1; ▲, measured values).

flow in the reactor inlet. Therefore, the predicting capability of the model can be judged by the shape of the temperature profile in the reactive zone of the reactor.

Table 6 shows calculated values of the heat and mass transfer coefficients. The estimated values for gas- and liquid-side mass transfer coefficients are in the range of the values of Metaxas and Papayannakos,[19] which were measured in a bench-scale reactor. Their measured liquid-side mass transfer coefficients were in the range of 0.005−0.3 s^{-1} for hydrogen and 0.001−0.1 s^{-1} for benzene. Most of the values were scattered between 0.01

Table 7. Liquid-Side Mass Transfer Coefficients Calculated with Different Correlations for Case 1

compd	$K_{Li,eff}a_{GL}$ (s^{-1}) inlet	outlet
Goto and Smith[15] Correlation		
H_2	0.0428	0.0473
benzene	0.0326	0.0362
cyclohexane	0.0312	0.0356
Wild et al.[26] High Interaction Regime		
H_2	1.03	1.15
benzene	0.852	0.956
cyclohexane	0.825	0.925
Wild et al.[26] Transition Regime		
H_2	0.0473	0.0434
benzene	0.0511	0.0467
cyclohexane	0.0517	0.0473
Turek and Lange[25] Correlation		
H_2	0.0017	0.0017
benzene	0.0013	0.0013
cyclohexane	0.0012	0.0013

and 0.05 s^{-1} for hydrogen and 0.005 and 0.02 s^{-1} for benzene. The measured gas-side mass transfer coefficients were in the range of 0.01−50 s^{-1} for hydrogen and 0.005−5 s^{-1} for benzene. This agreement seems contradictory to the usual statement that mass transfer coefficients are much smaller in bench-scale reactors than in industrial reactors.[3,9] Metaxas and Papayannakos[19] also found that virtually all correlations underestimate mass transfer coefficients at low gas and liquid superficial velocities.

Figure 3 shows hydrogen concentrations in the gas and liquid phases and on the catalyst surface. The difference between hydrogen concentration in the liquid phase and on the catalyst surface is almost negligible, compared to the difference in hydrogen concentration at the liquid side of the gas−liquid interface and in the liquid bulk phase. Figure 4 shows the volumetric hydrogen mass transfer and reaction rates and the benzene concentration in the liquid phase. The peaks in the liquid and surface hydrogen concentrations and the reaction rates at the inlet are due to the small amount of dissolved hydrogen that comes with the recycle stream. These cannot be compared due to lack of temperature measurements. In the model, there is no mixing of gas and liquid before the reactor inlet. In reality, gas and liquid are contacted at the liquid distributor before the reactive section, where some gas−liquid mass transfer may already take place. However, below the region very close to the feed, the effect of this mixing on the simulation results is negligible.

The importance of the liquid-side mass transfer resistance is further illustrated in Figures 5 and 6, which show results from sensitivity analysis simulations of case 1 where the values of $k_{LSi,eff}a$ have been scaled to 50% and 200% and $k_{Li,eff}a$ to 50%, 200%, 300%, and 500% of their original values, which were estimated with the Goto and Smith[15] correlations. Results with scaled $k_{Gi,eff}a$ values are not shown, since this did not have any effect on the results. The results show clearly that changes in the liquid-side mass transfer coefficient have the greatest impact on the simulation. The 300% curve shows another interesting phenomenon, namely, the transfer from mass-transfer-controlled to kinetically controlled reaction. This can be seen in the way the curve flattens smoothly. Now there is excess hydrogen present on the catalyst surface. The adsorption of hydrogen is so strong that it covers almost all the active sites, so that the rate of reaction is decreased. This is typical for this class of kinetics that is controlled by competitive adsorption of the reactants. This effect is even more pronounced in the 500% line. There seems to be an optimum for hydrogen mass transfer, at which the hydrogen concentration at the surface is close to zero and the reaction rate is the highest. The main parameters affecting gas−liquid mass transfer are liquid flow rate and particle size; these can be varied to find an optimal mass transfer coefficient. On a side note, the present reactor seems to be working under near-optimal conditions, since the hydrogen concentration at the surface is close to zero, as shown in Figure 3.

Figure 7 shows temperature profiles with the liquid-side mass transfer coefficient calculated with some popular correlations, namely, Goto and Smith,[15] Turek and Lange,[25] and Wild et al.[26] correlations. Table 7 shows the numerical values at the inlet and outlet of the reactor. The Turek and Lange[25] correlation clearly predicts too-low values. Judging from the figure, the Wild et al.[26] correlation for the high interaction regime seems to yield good results. However, the values calculated with the Wild et al.[26] correlation for the high interaction regime are approximately 20 times higher than the values from the Goto and Smith[15] correlation. In this case the reaction is kinetically

Table 8. Mass Transfer Correlations Used in This Work[a]

correlation	comments
Goto and Smith[15] (all flow regimes)	
$k_La\ (s^{-1}) = 10^4\alpha_L[D\ (m^2\cdot s^{-1})][10^{-2}G_L\ (kg\cdot m^{-2}\cdot s^{-1})/\mu_L\ (Pa\cdot s)]^{n_L}[Sc_L]^{0.5}$	
$\alpha_L = -2623d_p\ (m) + 13.63$	for $d_p > 0.0291$ m
$n_L = -8.197d_p\ (m) + 0.4339$	for $d_p > 0.0291$ m
$\alpha_L = -759.8d_p\ (m) + 8.211$	for $d_p \le 0.0291$ m
$n_L = 8.442d_p\ (m) + 0.3854$	for $d_p \le 0.0291$ m
Wild et al.[26]	
$Sh_L' = 2.8 \times 10^{-4}\{X_G^{0.5}Re_L^{0.8}We_L^{0.2}Sc_L^{0.5}[a_Sd_h/[1-\varepsilon]]^{0.25}\}^{3.4}$	low interaction flow regime
$Sh_L' = 0.091\{X_G^{0.25}Re_L^{0.2}We_L^{0.2}Sc_L^{0.3}[a_Sd_h/[1-\varepsilon]]^{0.25}\}^{3.8}$	transition flow regime
$Sh_L' = 0.45\{X_G^{0.5}Re_L^{0.8}We_L^{0.2}Sc_L^{0.5}[a_Sd_h/[1-\varepsilon]]^{0.25}\}^{1.3}$	high interaction flow regime
Turek and Lange[25]	
$k_La\ (s^{-1}) = 16.8 \times 10^4[D\ (m^2\cdot s^{-1})]Ga_L^{-0.22}Re_L^{0.25}Sc_L^{0.5}$	all regimes [$Re_L < 1$]
Yaici et al.[16]	
$Sh_Gad_p/[1-\beta] = 0.03\phi^{-1.56}Re_L^{0.33}Re_G^{0.87}Sc_G^{0.5}[d_p/d_R]^{-0.67}$	all regimes
Goto and Smith[15] (all flow regimes)	
$k_{LS}a\ (s^{-1}) = 10^4\alpha_S[D\ (m^2\cdot s^{-1})][10^{-2}G_L\ (kg\cdot m^{-2}\cdot s^{-1})/\mu_L\ (Pa\cdot s)]^{n_S}[Sc_L]^{1/3}$	
$\alpha_S = -57\,780d_p\ (m) + 184.3$	
$n_S = -58.86d_p\ (m) + 0.7018$	

[a] Dimensional equations have been converted into SI units (shown in parentheses).

limited, and the excess hydrogen is slowing the reaction. The situation is similar to the 500% curve in Figure 6. The further increase from 5- to 20-fold liquid-side mass transfer coefficient has very little effect, since the reaction is already completely kinetically limited. The Wild et al.[26] correlation for the transition regime, however, predicts values quite close to the Goto and Smith[15] correlation, and the predicted temperature profiles are qualitatively similar. Table 8 lists all correlations referred to in this work.

Goto and Smith[15] derived their correlation from absorption and desorption experiments of oxygen in water at liquid loadings (mass flow rate divided by reactor cross-section) comparable to industrial reactors. Turek and Lange[25] performed absorption experiments of hydrogen in cumene at much lower flow rates. They operated their reactor clearly in the low interaction regime, whereas the conditions in the reactor of Goto and Smith[15] were probably closer to the high interaction regime due to high liquid loading (between 1 and 8 $kg \cdot m^{-2} \cdot s^{-1}$). This similarity of the flow conditions may explain the good performance of the Goto and Smith[15] correlation. The Wild et al.[26] correlations were fitted to a wide experimental database compiled from literature. The correlation for the transition flow regime seems to yield acceptable results, but as discussed above, determination of the flow regime may be difficult, as there is no reliable correlation. The correlation for the high interaction regime is considered the most unreliable by the authors, since there were only limited data available from such systems.[26]

Turek and Lange[25] also performed experiments with hydrogenation of α-methylstyrene and found that mass transfer coefficients in the reactive system were considerably higher than in the absorption system, which is consistent with the observations of Metaxas and Papayannokos.[19] Turek and Lange[25] concluded that the application of mass transfer coefficients obtained from absorption measurements in modeling heterogeneous catalytic processes is problematic. They speculated that this could be due to the static liquid holdup, which is almost saturated with gas, and therefore does not contribute to the active interfacial area. Under reactive conditions, however, the gas is consumed by the reaction and the whole area is available for mass transfer. Another reason could be the formation of microturbulences in the liquid film that decrease the thickness of the boundary layer. These microturbulences are caused by thermoconvection and back diffusion of the products that take place under reaction conditions. Our results, however, suggest that it is possible to use data obtained from absorption systems for the design and scale-up of reactive systems if the data were collected in the transition or high interaction regime: In future experimental work, special attention should be given to the flow regime and a proper characterization of the hydrodynamics of the system under consideration.

Conclusions

In trickle-bed reactors, laboratory or industrial, gas−liquid mass transfer is the limiting phenomenon that controls the reaction rate. Therefore, accurate modeling of gas−liquid mass transfer is of great importance when designing trickle-bed reactors, and validated correlations for the mass transfer coefficients should be used. We have used temperature profile data from an industrial benzene hydrogenation reactor for testing of the trickle-bed reactor model with interfacial mass transfer by Toppinen et al.[4] The model was tested by comparing simulated reactor temperature profiles to the measurements. The simulation was able to reproduce the measured temperature profiles. Analysis of the simulation results shows that the process is limited by hydrogen mass transfer through the gas−liquid interface. Therefore the mass transfer correlations, especially for k_La, must be carefully chosen. Changes in k_La values are clearly pronounced in the simulated temperature profile, making an indirect validation of mass transfer correlations possible. The Goto and Smith[15] correlation, although it is the oldest of the tested correlations, yielded the best results. A possible explanation is that the correlation was derived from data gathered under similar hydrodynamic conditions (flow regime) as are encountered in the studied industrial reactor. Moreover, the estimated k_La and k_Ga values corresponded well to measurements by Metaxas and Papayannokos.[19] The comparison of our results with the experiments of Metaxas and Papayannakos[19] and Turek and Lange[25] suggests that mass transfer coefficients under reactive conditions are comparable in bench-scale and industrial trickle-bed reactors.

So far, there has been little validation data for mass transfer correlation in trickle-bed reactors under industrial operating conditions. On the basis of our study, we may recommend a combination of the Goto and Smith[15] correlations and the Yaici et al.[16] correlation for industrial trickle-bed design.

Acknowledgment

The Graduate School in Chemical Engineering is acknowledged for financial support.

Nomenclature

a_{GL} = gas−liquid mass transfer area/reactor volume (m^{-1})
a_{LS} = catalyst surface mass transfer area/reactor volume (m^{-1})
a_S = external area of particles and wall per unit reactor volume [$= 6(1 - \varepsilon)/\varphi d_p + 4/d_R$] ($m^{-1}$)
a_W = reactor wall heat transfer area/reactor volume (m^{-1})
c_i = concentration of component i ($mol \cdot m^{-3}$)
c_t = total concentration ($mol \cdot m^{-3}$)
$Đ_{ij}$ = Maxwell−Stefan diffusion coefficient of component pair $i-j$ ($m^2 \cdot s^{-1}$)
$D_{i,eff}$ = effective diffusivity of component i ($m^2 \cdot s^{-1}$)
d_h = Krischer and Kast hydraulic diameter [$= d_p\{16\varepsilon^3/9\pi(1 - \varepsilon)^2\}^{1/3}$] (m)
d_p = particle diameter (m)
d_R = reactor diameter (m)
E_a = activation energy ($kJ \cdot mol^{-1}$)
$\dot{E}_G$ = heat flow of gas phase (kW)
$\dot{E}_L$ = heat flow of liquid phase (kW)
g = gravitational acceleration ($m \cdot s^{-2}$)
G_L = liquid loading ($kg \cdot m^{-2} \cdot s^{-1}$)
Ga_L = liquid Galileo number [$= d_p^3 g \rho_L^2/\mu_L^2$]
$\bar{H}_{Gi}$ = partial molar enthalpy of component i in gas phase ($kJ \cdot mol^{-1}$)
$\bar{H}_{Li}$ = partial molar enthalpy of component i in liquid phase ($kJ \cdot mol^{-1}$)
k_1 = reaction rate constant at reference temperature ($mol \cdot s^{-1} \cdot kg^{-1}$)
k = mass transfer coefficient ($m \cdot s^{-1}$)
$k_{i,eff}$ = effective mass transfer coefficient of component i ($m \cdot s^{-1}$)
K = partition coefficient (dimensionless)
K_i = adsorption constant of component i ($m^3 \cdot mol^{-1}$)
K_i^* = vaporization equilibrium constant of component i (dimensionless)
n = number of components
$\dot{n}_{Gi}$ = gas molar flow of component i ($mol \cdot s^{-1}$)
$\dot{n}_{Li}$ = liquid molar flow of component i ($mol \cdot s^{-1}$)
n_L = parameter in Goto and Smith mass transfer correlation (dimensionless)
n_S = parameter in Goto and Smith mass transfer correlation (dimensionless)
N_{GLi} = gas−liquid mass transfer flux of component i ($mol \cdot m^{-2} \cdot s^{-1}$)

N_{LSi} = liquid−solid mass transfer flux of component i (mol·m^{-2}·s^{-1})
P = pressure (kPa)
q_{GL} = gas−liquid heat flux (kW·m^{-2})
q_{LS} = liquid−solid heat flux (kW·m^{-2})
q_W = liquid−wall heat transfer flux (kW m^2 s^{-1})
r_i = generation rate of component i (mol·s^{-1}·m^3)
R = reaction rate (mol s^{-1} kg^{-1}), gas constant (J·mol^{-1}·K^{-1})
Re_G = gas Reynolds number [$= u_G\rho_G d_p/\mu_G$]
Re_L = liquid Reynolds number [$= u_L\rho_L d_p/\mu_L$]
S = surface area of single catalyst particle (m^2)
Sc_G = gas Schmidt number [$= \mu_G/D_G\rho_G$]
Sc_L = liquid Schmidt number [$= \mu_L/D_L\rho_L$]
Sh_G = gas Sherwood number [$= k_L a d_p^2/D_G$]
Sh_L' = modified liquid Sherwood number in Wild et al. correlation [$= k_L a d_h^2/D_L$]
T_0 = reference temperature (K)
T_G = gas temperature (K)
T_I = temperature at gas−liquid interface (K)
T_L = liquid temperature (K)
T_S = catalyst surface temperature (K)
u_G = gas superficial velocity (m·s^{-1})
u_L = liquid superficial velocity (m·s^{-1})
V_R = volume of reactor (m^3)
We_L = liquid phase Weber number [$= u_L^2 d_p\rho_L/\sigma_L$]
X_G = Lockhart−Martinelli number [$= u_G\sqrt{\rho_G}/u_L\sqrt{\rho_L}$]
x_i = mole fraction of component i in liquid phase
y_i = mole fraction of component i in gas phase
z = reactor length (m)

Greek Symbols

α_G = gas film heat transfer coefficient (kW·m^2·K^{-1})
α_L = liquid film heat transfer coefficient (kW·m^2·K^{-1}), parameter in Goto and Smith correlation (dimensionless)
α_{LS} = heat transfer coefficient of liquid film surrounding catalyst (kW·m^2·K^{-1})
α_S = parameter in Goto and Smith correlation (dimensionless)
β = liquid holdup (dimensionless)
ε = catalyst bed void fraction (dimensionless)
φ = sphericity (dimensionless)
ρ_G = gas density (kg·m^{-3})
ρ_L = liquid density (kg·m^{-3})
μ_G = gas viscosity (Pa·s)
μ_L = liquid viscosity (Pa·s)
ϕ = shape factor in the correlation of Yaici et al. [$= S/d_p^2$; here a value of 4.7, according to an ideal cylinder, was assumed]
ξ = reactor length coordinate (dimensionless)

Subscripts and Superscripts

B = benzene
eff = effective
G = gas phase
GL = gas−liquid
H = hydrogen
i = component i
I = interface
j = component j
L = liquid phase
LS = liquid−solid
S = solid phase (catalyst)

Literature Cited

(1) Henry, H. C.; Gilbert, J. B. Scale Up of Pilot Plant Data for Catalytic Hydroprocessing. *Ind. Eng. Chem. Process Des. Dev.* **1973**, *12*, 328.

(2) Iannibello, A.; Marengo, S.; Burgio, G.; Baldi, G.; Sicardi, S.; Specchia, V. Modeling the Hydrotreating Reactions of a Heavy Residual Oil in a Pilot Trickle-Bed Reactor. *Ind. Eng. Chem. Process Des. Dev.* **1985**, *24*, 531.

(3) Korsten, H.; Hoffmann, U. Three-Phase Reactor Model for Hydrotreating in Pilot Trickle-Bed Reactors. *AIChE J.* **1996**, *42*, 1350.

(4) Toppinen, S.; Aittamaa, J.; Salmi, T. Interfacial mass transfer in trickle-bed reactor modelling. *Chem. Eng. Sci.* **1996**, *51*, 4335.

(5) Avraam,; D, G.; Vasalos, I. A. HdPro: a mathematical model of trickle-bed reactors for the catalytic hydroprocessing of oil feedstocks. *Catal. Today.* **2003**, *79*−*80*, 275.

(6) Murali, C.; Voolapalli, R. K.; Ravichander, N.; Gokak, D. T.; Choudary, N. V. Trickle bed reactor model to simulate the performance of commercial diesel hydrotreating unit. *Fuel* **2007**, *86*, 1176.

(7) Rajashekharam, M. V.; Jaganathan, R.; Chaudhari, R. V. A trickle-bed reactor model for hydrogenation of 2,4-dinitrotoluene: experimental verification. *Chem. Eng. Sci.* **1998**, *53*, 787.

(8) Nijhuis, T. A.; Dautzenberg, F. M.; Moulijn, J. A. Modeling of monolithic and trickle-bed reactors for the hydrogenation of styrene. *Chem. Eng. Sci.* **2003**, *58*, 1113.

(9) Bhaskar, M.; Valavarasu, G.; Sairam, B.; Balaraman, K. S.; Balu, K. Three-Phase Reactor Model to Simulate the Performance of Pilot-Plant and Industrial Trickle-Bed Reactors Sustaining Hydrotreating Reactions. *Ind. Eng. Chem. Res.* **2004**, *43*, 6654.

(10) Keskinen, K. I.; Aittamaa, J. Manual of the program FLOWBAT. http://www.tkk.fi/Units/ChemEng/WebFlowbat/FlowManual/Manuaali.doc.

(11) Wilke, C. R. Diffusional properties of multicomponent gases. *Chem. Eng. Prog.* **1950**, *46*, 95.

(12) Vignes, A. Diffusion in Binary Solutions. *Ind. Eng. Chem. Fundam.* **1966**, *5*, 189.

(13) Kooijman, H. A.; Taylor, R. Estimation of Diffusion Coefficients in Multicomponent Liquid Systems. *Ind. Eng. Chem. Res.* **1991**, *30*, 1217.

(14) Wilke, C. R.; Chang, P. Correlation of Diffusion Coefficients in Dilute Solutions. *AIChE J.* **1955**, *1*, 264.

(15) Goto, S.; Smith, J. M. Trickle-bed reactor performance. Part I. Holdup and mass transfer effects. *AIChE J.* **1975**, *21*, 706.

(16) Yaici, W.; Laurent, A.; Midoux, N.; Charpentier, J.-C. Determination of gas-side mass transfer coefficients in trickle-bed reactors in the presence of an aqueous or an organic liquid phase. *Int. Chem. Eng.* **1988**, *28*, 299.

(17) Chilton, T. H.; Colburn, A. P. Mass Transfer (Absorption) Coefficient. Prediction from Data on Heat Transfer and Fluid Friction. *Ind. Eng. Chem.* **1934**, *26*, 1183.

(18) Graboski, M. S.; Daubert, T. E. A Modified Soave Equation of State for Phase Equilibrium Calculations. 1. Hydrocarbon Systems. *Ind. Eng. Chem. Process Des. Dev.* **1978**, *17*, 443.

(19) Metaxas, K. C.; Papayannakos, N. G. Kinetics and Mass Transfer of Benzene Hydrogenation in a Trickle-Bed Reactor. *Ind. Eng. Chem. Res.* **2006**, *45*, 7110.

(20) Toppinen, S.; Rantakylä, T.-K.; Salmi, T.; Aittamaa, J. Kinetics of the Liquid-Phase Hydrogenation of Benzene and Some Monosubstituted Alkylbenzenes over a Nickel Catalyst. *Ind. Eng. Chem. Res.* **1996**, *35*, 1824.

(21) Sáez, A. E.; Carbonell, R. G. Hydrodynamic Parameters for Gas-Liquid Cocurrent Flow in Packed Beds. *AIChE J.* **1985**, *31*, 52.

(22) Ellman, M. J.; Midoux, N.; Laurent, A.; Charpentier, J. C. A New, Improved Liquid Hold-Up Correlation for Trickle-Bed Reactors. *Chem. Eng. Sci.* **1990**, *45*, 1677.

(23) Larachi, F.; Laurent, A.; Wild, G.; Midoux, N. Effet de la pression sur la transition ruisselant-pulsé dans les réacteurs catalytiques à lit fixe arrosé. *Can. J. Chem. Eng.* **1993**, *71*, 319.

(24) Urseanu, M. I.; Boelhouwer, J. G.; Bosman, H. J. M.; Schroijen, J. C.; Kwant, G. Estimation of trickle-to-pulse flow regime transition and pressure drop in high-pressure trickle-bed reactors with organic liquids. *Chem. Eng. J.* **2005**, *111*, 5.

(25) Turek, F.; Lange, R. Mass transfer in trickle-bed reactors at low Reynolds number. *Chem. Eng. Sci.* **1981**, *36*, 569.

(26) Wild, G.; Larachi, F.; Charpentier, J. C. Heat and mass transfer in gas-liquid-solid fixed bed reactors. In *Heat and Mass Transfer in Porous Media*; Quintard, M., Todorovic, M., Eds.; Elsevier: Amsterdam, 1992.

Received for review September 19, 2008
Revised manuscript received November 6, 2008
Accepted November 12, 2008

IE801411N